RSC Advances

PAPER

View Article Online
View Journal | View Issue

Cite this: *RSC Adv.*, 2016, **6**, 115271

Pro-oxidant effects of nano-TiO_2 on *Chlamydomonas reinhardtii* during short-term exposure†

Nadia von Moos,*[a] Volodymyr B. Koman,[b] Christian Santschi,*[b] Olivier J. F. Martin,[b] Lionel Maurizi,‡[c] Amarnath Jayaprakash,[c] Paul Bowen[c] and Vera I. Slaveykova*[a]

Received 28th June 2016
Accepted 1st December 2016

DOI: 10.1039/c6ra16639c

www.rsc.org/advances

This study sheds light on the short-term dynamics of pro-oxidant processes related to the exposure of *C. reinhardtii* microalgae to nano-TiO_2 using (a) conventional fluorescence probes for cellular pro-oxidant process and (b) a recently developed cytochrome c biosensor for the continuous quantification of extracellular H_2O_2. The main aims are to investigate nano-TiO_2 toxicity and the modifying factors thereof based on the paradigm of oxidative stress and to explore the utility of extracellular H_2O_2 as a potential biomarker of the observed cellular responses. This is the first study to provide continuous quantitative data on abiotic and biotic nano-TiO_2-driven H_2O_2 generation to systematically investigate the link between extracellular and cellular pro-oxidant responses. Acute exposures of 1 h were performed in two different exposure media (MOPS and lake water), with nominal particle concentrations from 10 mg L^{-1} to 200 mg L^{-1}, with and without UV pre-illumination. Abiotic and biotic extracellular H_2O_2 were continuously measured with the biosensor and complemented with endpoints for abiotic ROS (H_2DCF-DA), oxidative stress (CellROX® Green) and damage (propidium iodide) measured by flow cytometry at the beginning and end of exposure. Results showed that nano-TiO_2 suspensions generated ROS under UV light (abiotic origin) and promoted ROS accumulation in *C. reinhardtii* (biotic origin). However, extracellular and intracellular pro-oxidant processes differed. Hence, extracellular H_2O_2 cannot *per se* serve as a predictor of cellular oxidative stress or damage. The main predictors best describing the cellular responses included "exposure medium", "exposure time", "UV treatment" as well as "exposure concentration".

Introduction

With the increasingly pervasive use of engineered nanomaterials (ENMs) in modern society, the aquatic system has been recognized as a primary environmental entry point and sink for ENMs inevitably discharged by anthropogenic activity.[1–3] Yet, the associated inadvertent implications for the overall ecotoxicological risk remain uncertain.[3–6] The ability of inorganic nanoparticles to generate reactive oxygen species (ROS) and thereby cause oxidative stress and damage is currently one of the most well developed paradigms to explain their biological effects[5,7–15] even though to date the underlying mechanisms are not yet fully understood and the particle *vs.* ion dilemma persists.[16,17]

Thus, an in-depth understanding of normal and ENM-stimulated ROS production as well as antioxidant levels can improve our understanding of the potential hazards related to ENMs.

More than a decade ago, Livingstone[18] identified the following key challenges of aquatic toxicology for improved risk assessment: (i) identification of pro-oxidant species, (ii) design of novel toxicity assays for the detection of pro-oxidant activity, (iii) quantitative assessment of contaminant-mediated pro-oxidant processes compromising biological fitness and lastly (iv) identification of environmental and biological factors that modulate ENM-stimulated ROS generation and oxidative damage.[18]

Against this background, the purpose of the present research study is twofold: firstly, it assesses the effect of nano-TiO_2 to the model aquatic microalga *Chlamydomonas reinhardtii* by

[a]*Environmental Biogeochemistry and Ecotoxicology, Department F.-A. Forel for Environmental and Aquatic Sciences, School of Earth and Environmental Science, University of Geneva, Uni Carl Vogt, 66, Bvd. Carl Vogt, CH-1211 Geneva 4, Switzerland. E-mail: nadia.vonmoos@epfl.ch; nadia.vonmoos@immerda.ch; vera.slaveykova@unige.ch; Tel: +41 22 397 0335*

[b]*Nanophotonics and Metrology Laboratory, Swiss Federal Institute of Technology Lausanne (EPFL), CH-1015 Lausanne, Switzerland*

[c]*Powder Technology Laboratory, Institute of Materials, Swiss Federal Institute of Technology Lausanne (EPFL), CH-1015 Lausanne, Switzerland; christian.santschi@epfl.ch; Tel: +41 21 69 36902*

† Electronic supplementary information (ESI) available. See DOI: 10.1039/c6ra16639c

‡ Current address: Laboratoire Interdisciplinaire Carnot de Bourgogne, UMR 6303 CNRS-Université, Bourgogne Franche-Comté, 9 Av. A. Savary, BP 47870, F-21078 DIJON Cedex, France.

investigating its pro-oxidant potential and possible modifying factors thereof by well-established fluorescent probes for oxidative stress and damage. These cellular endpoints were complemented with nano-TiO_2-induced abiotic ROS measured by H_2DCF-DA fluorescence.

Secondly, this is the first in-depth, systematic nano-ecotoxicological study to use extracellular H_2O_2 concentrations as a complementary endpoint in achieving the first aim, in an attempt to validate this recently developed method based on a cytochrome c biosensor.[19–22] Unlike other approaches applied in nanotoxicity testing, this biosensor is non-invasive and provides quantitative measurements of extracellular H_2O_2 concentrations in real time. Stress-induced H_2O_2 can rapidly diffuse across the plasma membrane, passively or through aquaporin channels[23,24] and can be detected from as early as a few seconds to as long as a few days after stress application,[25] making it a suitable indicator for pro-oxidant responses in biological systems.[26] Here, we aim to evaluate to what extent extracellular H_2O_2 can serve as a biomarker for oxidative stress and damage in cells exposed to nano-TiO_2.

For this purpose, the microalga *C. reinhardtii* was exposed to two series of nano-TiO_2 suspensions at nominal concentrations of 10, 50, 100 and 200 mg L^{-1}, one of which previously received a 20 min UVA illumination, in two exposure media. These were a common laboratory testing buffer and lake Geneva water. In this way, we investigate the impact of the factors "exposure medium", "exposure concentration", "exposure time" and "UV treatment" on the pro-oxidant potential of nano-TiO_2.

The microalga *C. reinhardtii* represents one of the most sensitive classes of aquatic microorganisms to metal oxide ENMs[27] that can serve as early sentinel for potential environmental hazards in aquatic systems.[28]

Nano-TiO_2 is the most abundantly produced, most widely applied and investigated ENM that assumes the role of a benchmark against which other particles can be compared.[29] Most common applications are in the fields of photovoltaics, photocatalysis and sensing but also include its use as a white pigment in paints, cosmetics, personal care products and as E-171 in food.[30–33] As a semiconductor, energies equal to or higher than its band gap around 3.2 eV (photons with wavelengths < 385 nm) generate electron–hole pairs (h_{VB}^{+}/e_{CB}^{-}) on its surface that, by reacting with surface H_2O and O_2 in aqueous media, drive the formation of various ROS. These ROS include superoxide anions ($O_2^{\bullet -}$), hydrogen peroxide (H_2O_2), free hydroxyl radicals ($OH^{\bullet}$) and singlet oxygen ($^1O_2$).[34–37] With reported EC_{50} values of nano-TiO_2 for microalgae broadly varying from approximately 5 mg L^{-1} to 241 mg L^{-1},[38] nano-TiO_2 is one of the less toxic ENMs.[5] An augmented photocatalytic inhibition of algae is known[39] but it has been shown that ROS mediated nano-TiO_2 toxicity on microalgae also occurs in normal light conditions and does not significantly differ from UV treatments.[40–43]

Materials and methods

Experimental design

Experiments with algae were performed in two different exposure media and in two series of four different nano-TiO_2 concentrations (10, 50, 100 and 200 mg L^{-1}), one of which was performed with untreated particles and the other of which received a 20 min pre-illumination with long wave UV before contact with cells. Extracellular ROS was then monitored during 1 h with a novel portable oxidative stress sensor (POSS). To assess intracellular ROS levels and membrane integrity, the same exposure conditions were repeated separately and the samples stained with fluorescent probes for measurements by flow cytometry at the beginning of exposure ($t = 0$ h) and after 1 h ($t = 1$ h). All exposure conditions were replicated at least three times. All reagents (analytical grade) were purchased from Sigma Aldrich (Buchs, Switzerland), unless stated otherwise.

Algal culture

Axenic cultures of *Chlamydomonas reinhardtii* (CPCC 11) from the Canadian Phycological Culture Center (CPCC, Department of Biology, University of Waterloo, Canada) were grown in four times diluted Tris–Acetate–Phosphate (TAP × 4) liquid growth medium[44] and maintained in an incubator (Infors, Bottmingen, Switzerland) at 20 °C with a 24 h illumination regime (114.2 μmol phot per m^2 per s) and constant rotary shaking (100 rpm). The culture was regularly re-inoculated in fresh growth medium and cells were harvested in mid-exponential phase. For exposure experiments, cells were gently transferred to the respective exposure media by centrifugation (twice 805 g for 5 min, Sigma 3K10) and adjusted to a final concentration of approximately 10^6 cells per mL. All laboratory ware used for culturing was previously soaked in 5% v/v HNO_3 for at least 24 h, thoroughly rinsed with MilliQ water (MilliQ Direct system, Merck Millipore, Darmstadt, Germany) and sterilized in the autoclave (Steam Sterilizer, Nüve). All manipulations were performed in a sterile, laminar flow hood.

Exposure media

The exposure media included a 10^{-2} M solution of the Good's buffer 3-(*N*-morpholino)propanesulfonic acid (MOPS, pH = 7 ± 0.2) and Lake Geneva water (pH = 8.1 ± 0.2, physicochemical parameters provided in Table S1†). Surface lake water was sampled from Lake Geneva at 46.2824° N, 6.1661° E from *ca.* 1.5 m depth and filter sterilized (1.2 μm with a PolyPro XL cartridge filter and 0.22 μm with an Isopore Membrane). The MOPS buffer was prepared in MilliQ water, its pH adjusted with 65% HNO_3 and sterilized by autoclave and filtration (0.22 μm Isopore Membrane, polycarbonate, Hydrophilic). The sterile exposure media were stored in the dark at 4 °C.

UV treatment

Nano-TiO_2 suspensions received a 20 min illumination with long wave UV (300–420 nm = UVA) in the absorption range of nano-TiO_2 (λ < 385 nm)[45] before contact with algae. The intensity of the UV lamp (Waldmann Typ 602352 230 V 50 Hz 2 × 4 W) at the sample was 60 μW cm^{-2} nm^{-1}, at the wavelength 350 nm (Fig. S2†), which corresponds to an integrated intensity of 2700 μW cm^{-2} in the wavelength range 300–420 nm. This dose is in the range of intensities commonly occurring in natural aquatic environments.[46]

TiO_2 handling and characterization

A stock suspension of 2 g L^{-1} nano-TiO_2 (Degussa P25: 80% anatase, 20% rutile) was prepared in ultrapure water, sonicated in an ultrasonication bath for 10 min (Telsonic 150/300 W) and then stored at 4 °C in the dark for the duration of the experiments. Primary particle properties are provided in Fig. S1.† For exposure experiments, an intermediate working stock suspension was prepared by sonicating the initial stock suspension for 15 min in an ultrasonic water bath (Branson 2510) and then sampling an aliquot of 1 mL into an Eppendorf tube, which was stored in the dark at 4 °C for use within 1 d. Before every experiment, this intermediate stock suspension was retrieved, sonicated in an ultrasonic bath for 5 min directly before the preparation of the final, nominal exposure concentrations of 10, 50, 100 and 200 mg L^{-1} nano-TiO_2 within no more than 1 h. H_2O_2 concentrations measured in the supernatant of the unsonicated and sonicated stock suspension are provided in Fig. S8.†

For all exposure conditions the number-/volume-/intensity-weighted hydrodynamic particle diameter distributions and zeta potentials were measured by dynamic light scattering (DLS) and electrophoresis with a Zetasizer Nano ZS (Malvern Instruments) at the beginning and end of exposure to cells. This was performed in separate experiments, in suspensions without algae cells. Hence, non-UV suspensions were measured at $t = 0$ and $t = 60$ min after suspension preparation while UV-treated suspensions at $t = 20$ min (initial contact with cells) and $t = 80$ min after suspension preparation. Samples were measured in triplicates, consisting of approximately 10 runs each. The *z*-average particle diameters were derived by the method of cumulants and the zeta potential was derived from the electrophoretic mobility using the Smoluchowski approximation.

Particle sedimentation in the present exposure conditions was both experimentally determined and computationally estimated. In separate experiments using suspensions without algae, the supernatants of the nano-TiO_2 suspensions were measured after 1 h by ICP-MS (Elan DRC, Perkin Elmer). The "*In vitro* Sedimentation, Diffusion and Dosimetry" model, known as ISDD, was used for the computational estimation of particle sedimentation. The model was obtained from its developers[47] and is available as MatLab code or Windows Executable. The input parameters specific to our experimental setups are provided in Tables S2 and S3.† The model provides two alternative approaches for the calculation of agglomerate properties, one based on agglomerate diameter (*i.e.* by the Sterling equation) or one based on agglomerate density. Here, the Sterling approach was used, which uses the agglomerate diameter and fractal dimension (default = 2.3) to calculate agglomerate density, porosity and transport. The model yields the following four output values: (1) fraction of administered dose deposited (*i.e.* fraction of nominal dose sedimented), and the corresponding (2) total number of primary NPs deposited, (3) total SA (sphere) of primary NPs [cm^2] deposited and lastly (4) total mass [μg] deposited. A typical simulation did not exceed 1 minute of calculation time.

Extracellular pro-oxidant processes

Extracellular abiotic ROS. ROS in abiotic exposure conditions was qualitatively detected by the 2′,7′-dichlorofluorescin diacetate (H_2DCF-DA, D6883-250 MG, Sigma Aldrich) assay.[48,49] Before staining samples, the non-fluorescent dye was first dissolved in ethanol and then deacetylated by the addition of 0.01 M NaOH (pH = 7.2) in the dark, which yielded the H_2DCF molecule sensitive to oxidation. The deacetylation reaction was halted after 30 min by the addition of 0.1 M sodium phosphate (pH = 7.2) on ice in the dark. Finally, samples were aliquoted into 96-well plates and incubated with a final concentration of 26 μM H_2DCF for 30 min in the dark, after which fluorescence was measured in a plate reader (Tecan, Infinite M200) at 485/528 ± 20 nm. For positive controls, samples were spiked with 1 mM $FeSO_4$ (Sigma Aldrich) and 13 mM H_2O_2 (Sigma Aldrich). At least 3 × 3 replicates were prepared for every exposure condition and measured at the beginning ($t = 0$ h) and end of the exposure time ($t = 1$ h).

Quantification of extracellular abiotic and biotic peroxide. Extracellular H_2O_2 was measured with an optical, portable oxidative stress sensor (POSS), a non-invasive method recently described by Koman *et al.*[21,22] for the continuous quantification of H_2O_2 with an unprecedented limit of detection (LOD) in the tens of nanomolar range. The principal sensing element of the POSS consists of a ferrous heme group (Fe^{II}) embedded in the hemeprotein cytochrome c (cyt c), whose transmission spectrum at the wavelength $\lambda = 550$ nm conspicuously evolves from a sharp peak to a broad flat dip upon oxidation to ferric iron (Fe^{III}) and the simultaneous reduction of H_2O_2 to water. This transformation can be related to the concentration of oxidizing agents, such as H_2O_2, present in the sample. Optical measurements (in transmission mode) were performed in the reaction chamber, the core component of the POSS, consisting of an O-ring (8.0 mm × 1.0 mm, NBR Nitril, BRW) imperviously mounted onto a glass slide with grease (Dow Corning® high-vacuum silicone), forming a chamber with a volume of 60 μL to contain the sample and a cyt c spot, which is sealed with a cover slip. For every replicate, a new reaction chamber was prepared, filled with 80 μL of a freshly prepared sample, equipped with a freshly defrosted (fully reduced) cyt c spot, covered with a cover slip and excess liquid removed. Extracellular H_2O_2 was then continuously measured for 1 h, immediately after the initial contact of algae with TiO_2 (max. lag time 5 min.). At the end of every 1 h measurement, reference measurements of the background scattering were performed for every sample. Cyt c sensing spots were previously printed onto filtration membranes, as described in Koman *et al.*[21] and stored in in a freezer at −20 °C until use. Control measurements revealed that nano-TiO_2 suspensions did not affect the signal of the optical sensor (Fig. S3†). Calibration curves for H_2O_2 were prepared for both exposure media (Fig. S4†), yielding the required values of the interaction constant *k* for the derivation of H_2O_2 concentrations according to Koman *et al.*[21]

Cellular pro-oxidant processes. The cellular responses oxidative stress and membrane integrity were assessed by flow cytometry (FCM, BD Accuri C6, Accuri cytometers Inc., Michigan)

equipped with a multisampler (Accuri CSampler), a 488 nm argon excitation laser, three fluorescence detectors (FL 1-3) and respective software (BD Accuri C6 1.0.264.15) for data acquisition and analysis. The fluidics rate for sampling was set to slow (14 μL min^{-1}, core size 10 μm) and run limits were set to 20 000 events per sample (gated on algae in FL3). Details on the FCM gating strategy applied for data analysis are supplied in Fig. S5† and corresponds to that previously described.[17] For every exposure condition two aliquots of 250 μL were sampled at $t = 0$ h and $t =$ 1 h, which were stained with fluorescent probes (Invitrogen, Life Technologies) and incubated for 30 min prior measurements. Intracellular oxidative stress was assessed with the fluorescent probe CellROX® Green Reagent (CRG), which was added at a final concentration of 5 μM and analyzed with the green fluorescence detector FL1 (530 ± 15 nm). Positive controls for oxidative stress were obtained by exposing algae to 0.8 mM cumene hydroperoxide for 30 min before staining with CRG. Membrane integrity was evaluated with propidium iodide (PI), added at a final concentration of 7 μM and analyzed in the orange fluorescence detector FL2 (585 ± 20 nm). Positive controls for membrane damage were obtained by exposing cells to 1 M CH_2O for 30 min before adding PI.

Statistical analysis. Graphs were prepared with Origin Pro 8 and R version 3.1.3 "Smooth Sidewalk". For statistical analysis, FCM data was log-transformed and two obviously aberrant outliers were removed. Tukey box plots show the 1st, 2nd (median) and 3rd quartiles and the whiskers indicate the lowest and highest values within 1.5 times the interquantile range from the lower and upper quartile, respectively.

To analyze the underlying data generating factors of the discrete data sets obtained for abiotic ROS (measured by H_2DCF-DA), oxidative stress (CellROX® Green) and membrane integrity (propidium iodide) a linear regression model was fit with *R*, containing the main predictors "exposure medium", "exposure time", "exposure concentration" and "UV treatment" (medium + time + concentration + UV) and all their interactions (medium:time, medium:concentration *etc.*). Model selection was performed by the BIC (simple model) and AIC (complex, more predictive model, see ESI for definitions and details, Section 2.1†). Since abiotic ROS measurements and cellular endpoints have different units (fluorescence in a.u. and % affected cells, respectively), statistical analyses were performed separately. All *R* output tables and residual analyses are provided in the ESI (Tables S6–S16, Fig. S9 and S10†).

Results and discussion

Characterisation of nano-TiO_2 in exposure conditions

Hydrodynamic diameter (d_h). The measured intensity-weighted diameters indicate that nano-TiO_2 suspensions heavily agglomerated, immediately at the start of exposure in both exposure media and both treatments ($t_{initial}$ and $t_{initial\ UV}$). Even at the lowest concentration of 10 mg L^{-1} ($t_{initial}$), showing the least agglomeration, particle diameters already increased from the original 75 nm (primary size, Fig. S1†) up to diameters between 450 nm and 2500 nm (Fig. 1A and C) and continued to increase with increasing concentrations. Number and volume-weighted d_h are provided in the ESI (Fig. S6†) and showed similar trends (Fig. S7A and B†).

These hydrodynamic diameters are at the extreme limit of the DLS method and the measured sizes are unreliable but the trends seem to be consistent. What is more, the suspensions are polydisperse (polydispersity index largely between 0.3–0.5, Table S4†), in which case the assumptions underlying the DLS method are no longer fulfilled. Therefore, it makes little sense to discuss differences between concentrations and media in detail but the general trends can be summarized as follows: d_h increased with (i) nano-TiO_2 concentration (d_h (10 mg L^{-1}) < d_h (200 mg L^{-1})) and (ii) time (d_h ($t_{initial}$) < d_h (t_{final})) in both media (Fig. 1, S7C–F†).

Finally, there is one more interesting point we can extract from the data. Diameters were measured at the beginning and end of the 1 h exposure duration, in both treatments. Due to the 20 min pre-illumination period in the UV treatments, $t_{initial}$ and $t_{initial\ UV}$ as well as t_{final} and $t_{final\ UV}$ are 20 min apart (see method section) with respect to the moment of suspension preparation (reference point for 0 min), which yields us measured values at 0 min ($t_{initial}$), 20 min ($t_{initial\ UV}$), 60 min (t_{final}), 80 min ($t_{final\ UV}$) that provide some insight into agglomeration kinetics. First, the results indicate that the suspensions had not reached an equilibrium state in the investigated time period. Second, it is striking that diameters at $t_{final\ UV}$ (*i.e.* 80 min) seem to "decrease" again, especially in lake water settings. This suggests that sedimentation occurred in the, at this point, heavily agglomerated (n.b. polydisperse) suspensions. Thus, large agglomerate subpopulations were possibly removed from the water column, leaving behind smaller subpopulations only for detection by DLS.

All in all, particles in the present exposure system were no longer in the nanometer range but much larger sized agglomerates in the micrometer size range. For comparison, *C. reinhardtii* cells have diameters around 5–10 μm.

These findings are in agreement with earlier observations of nano-TiO_2 forming agglomerates of several hundred nanometers to several micrometers in diameter within minutes at environmentally relevant pH, ionic strengths and dissolved organic matter (DOM).[50,51] A comprehensive study investigating the behavior of nano-TiO_2 in natural matrices at the same concentrations employed here found very low sedimentation rates in freshwater suggesting ecotoxicologically relevant residence times of agglomerated nano-TiO_2 for aquatic organisms in the water column.[52]

Particle sedimentation. Experimental data suggest that 52–97% of the initially administered concentration of Ti sediments in the FCM setup within 1 h. The computational estimates suggest that after 1 h 1.5–1.7% of the administered dose deposits in the FCM setup and 6.8–8.5% in the biosensor setup (Table S5†). The experimental and computational results differ by one order of magnitude. The reality is likely to lie somewhere between.

Nonetheless, these findings suggest that particokinetics (particle transport) was similar in the two media. Also, the experimental results suggest that after 1 h the final concentration of Ti [mg L^{-1}] in the supernatant was somewhere in the

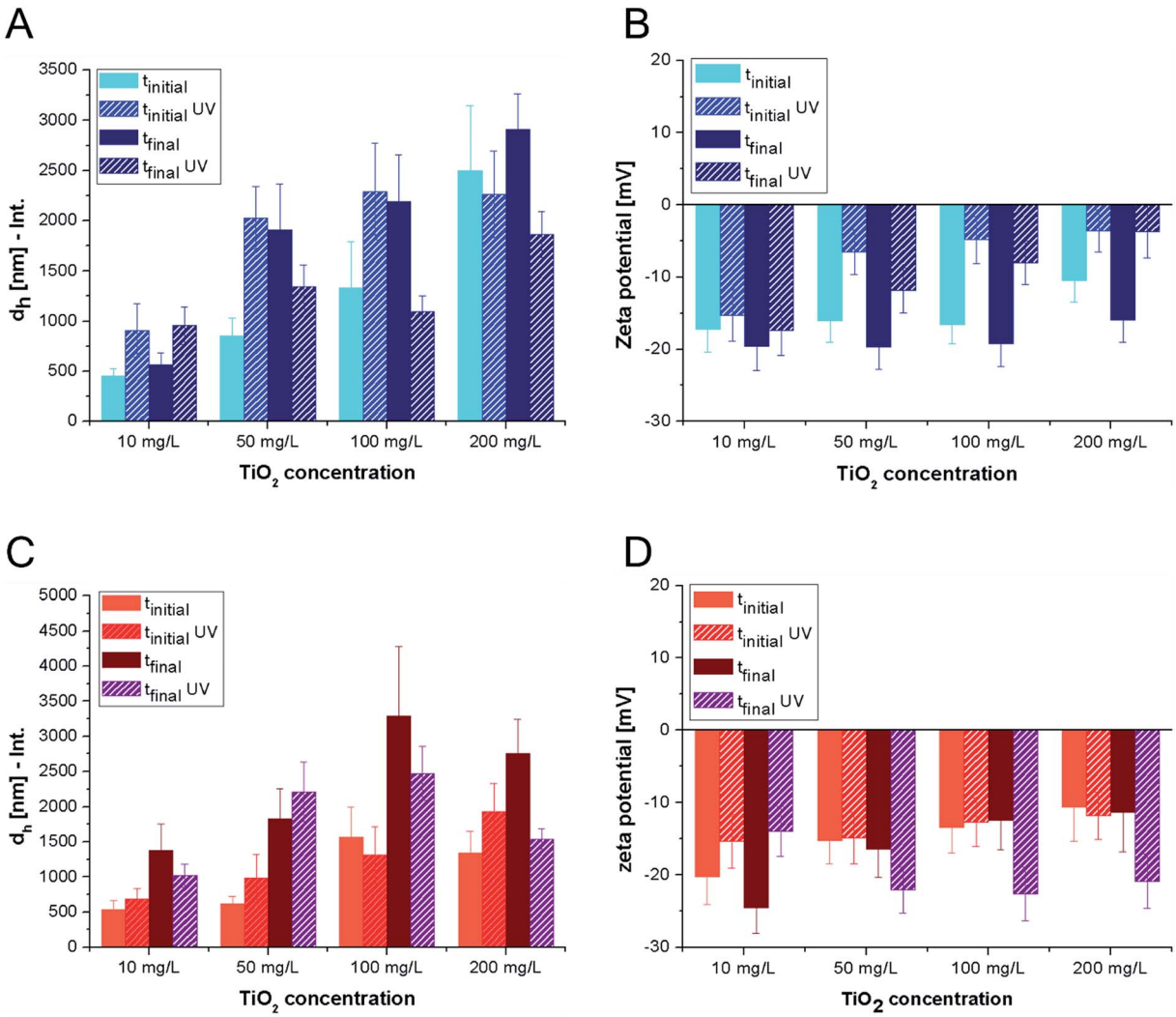

Fig. 1 Mean and standard deviation of intensity-weighted hydrodynamic diameters (d_h – Nb) (A, C) and zeta potentials (B, D) of different nominal nano-TiO_2 concentrations in lake water (A, B) and MOPS (C, D) at the beginning ($t_{initial}$) and end (t_{final}) of the 1 h exposure. Diameters for untreated samples correspond to times $t_{initial} = 0$ min and $t_{final} = 60$ min (after the preparation of the suspension). Diameters of UV pre-treated samples correspond to times $t_{initial\ UV} = 20$ min and $t_{final\ UV} = 80$ min after suspension preparation.

range of *ca.* 3–4 mg L^{-1} at all administered doses, except in MOPS (at a nominal dose of 200 mg L^{-1}), where the concentration of Ti in the supernatant was *ca.* 7 mg L^{-1} after 1 h.

Zeta potential. The zeta potential values of untreated particles in lake water lay between −20 mV and −15 mV and decreased in absolute value with increasing particle concentrations (Fig. S7E and F†), reaching values around −10 mV in the 200 mg L^{-1} suspension. The values were largely comparable at $t_{initial}$ and t_{final}.

Likewise, the zeta potential values in the MOPS buffer roughly varied between −20 mV and −10 mV. Zeta potentials at $t_{initial}$ and t_{final} remained more or less the same.

Cellular effects of nano-TiO_2 on *C. reinhardtii*

Oxidative stress in lake water. In lake water exposures the proportion of cells affected by oxidative stress did not exceed 5% (Fig. 2A and Table S6†) but intracellular ROS levels showed a concentration dependent increase after 1 h of exposure in both treatments, with highest responses obtained for algae exposed to 100 and 200 mg L^{-1} nano-TiO_2. UV minutely enhanced median intracellular ROS levels in lake water, leading to higher values at $t = 1$ h in [50 mg L^{-1}] UV and [100 mg L^{-1}] UV treatments (Fig. 2A and Table S6†). Controls and 10 mg L^{-1} nano-TiO_2 exposures produced comparable responses in both treatments (Fig. 2A).

Oxidative stress in MOPS. In the MOPS buffer, no effects on intracellular ROS levels were observed in neither of the two treatments (Fig. 3A and Table S7†). A marked increase in the proportion of cells with elevated intracellular ROS was observed in all conditions after 1 h, including the controls, suggesting that the MOPS medium may have acted as a stressor itself (Fig. 3A). The pre-irradiation of nano-TiO_2 with UV slightly reduced median intracellular ROS responses at all concentrations in the MOPS buffer.

Membrane integrity in lake water. Membrane damage predominantly occurred in lake water (Fig. 2B, Tables S12 and

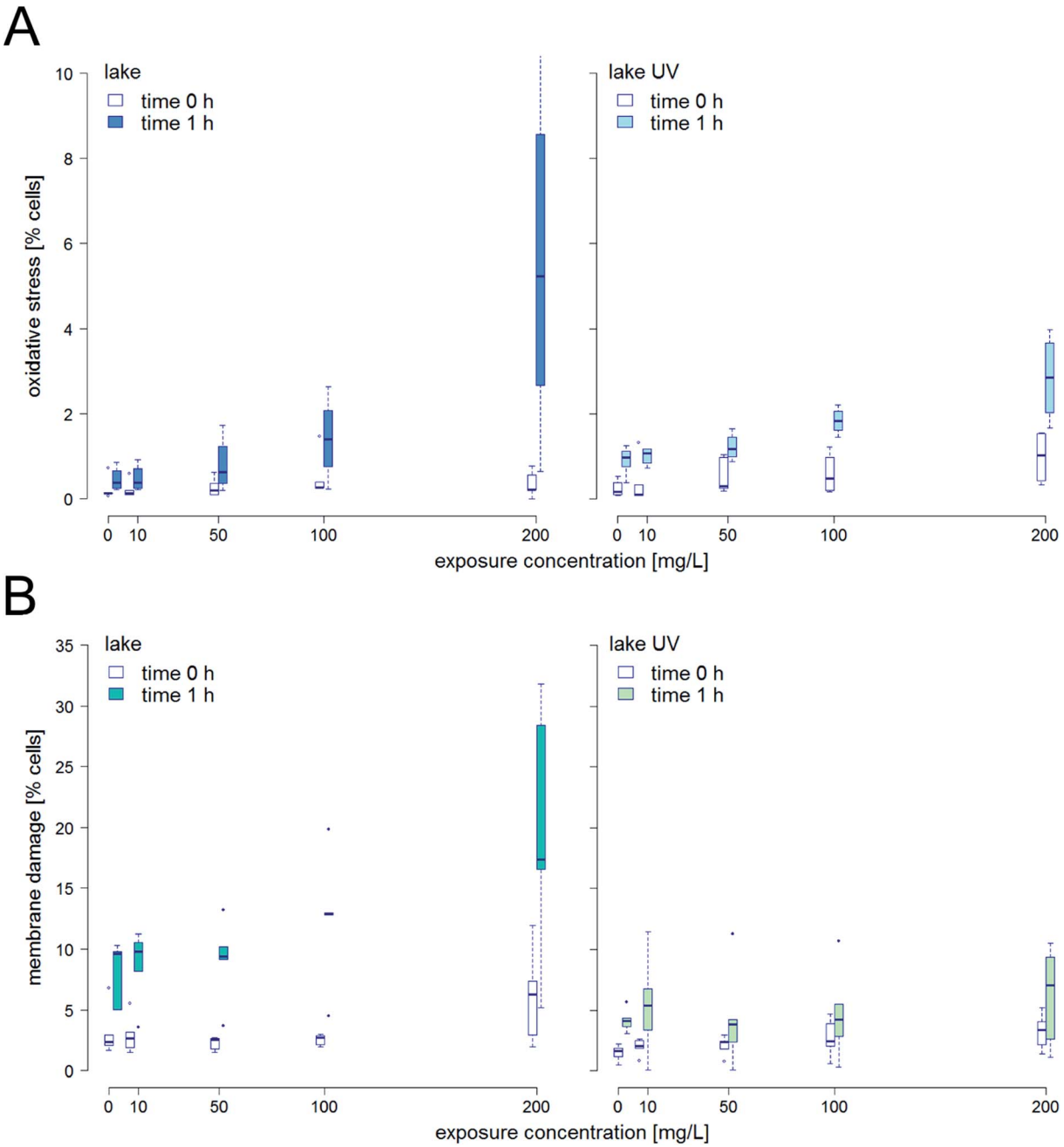

Fig. 2 Tukey box plots of $n = 5$ replicates showing intracellular ROS (A) and membrane damage (B) in [% affected cells] of the total number of cells exposed to 0 (negative control), 10, 50, 100 and 200 mg L^{-1} nano-TiO_2 concentrations without (left plot) and with UV pre-treatment (right plot) in lake water at the beginning ($t = 0$ h) and end of exposure ($t = 1$ h).

S13†) and the proportion of affected cells was more than one order of magnitude higher than in MOPS. In lake water, membrane impairment was considerably elevated in cells exposed to 100 and 200 mg L^{-1} nano-TiO_2 for 1 h reaching 12% and 19% affected cells, respectively, compared to *ca.* 8% in controls. There was no difference in membrane damage between controls and cells exposed to 10 mg L^{-1} and 50 mg L^{-1} nano-TiO_2 (Fig. 2B and Table S12†). UV pre-treated nano-TiO_2 did not greatly affect responses, but rather even decreased the proportion of affected cells (Fig. 5B).

Membrane integrity in MOPS. In MOPS the effects of nano-TiO_2 on the membrane integrity of *C. reinhardtii* were altogether negligible (<1%, Fig. 3B and Table S11†). No differences in membrane damage were observed between control and exposed cells but, opposed to results obtained for intracellular ROS, the membrane integrity of controls was not affected by the MOPS medium itself.

Overall, cellular responses were higher in lake water exposures, which is in agreement with earlier results showing a heightened toxicity of nano-TiO_2 on developing zebrafish in

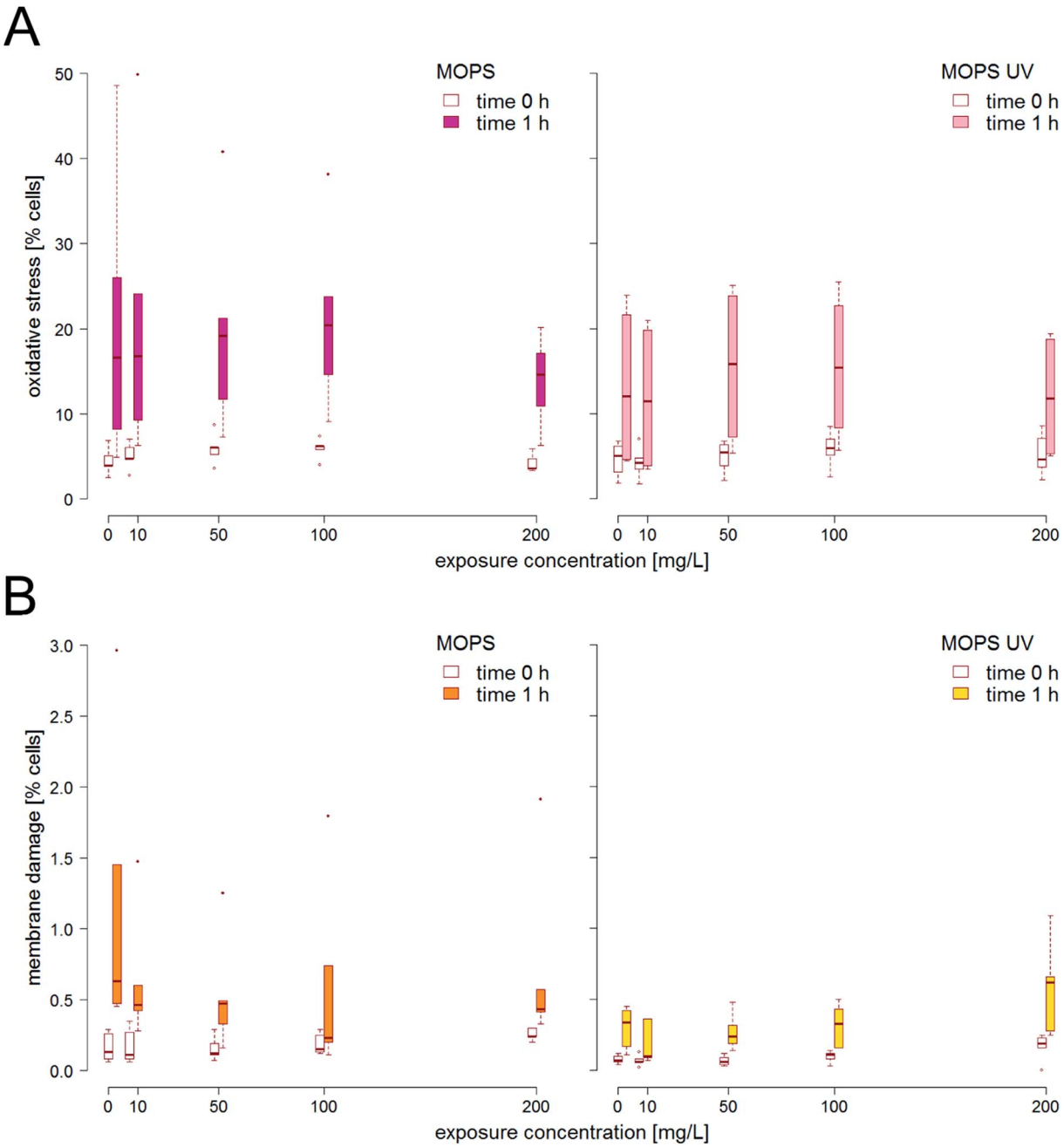

Fig. 3 Tukey box plots of $n = 5$ replicates showing intracellular ROS (A) and membrane damage (B) in [% affected cells] of the total number of cells exposed to 0 (negative control), 10, 50, 100 and 200 mg L^{-1} nano-TiO_2 concentrations without (left plot) and with UV pre-treatment (right plot) in the MOPS buffer at the beginning ($t = 0$ h) and end of exposure ($t = 1$ h).

the presence of humic acid[53] but contradicts others showing a mitigation of nano-TiO_2-induced pro-oxidant effects on the alga *Chlorella* sp. through increased electrosteric repulsion.[54]

Main predictors of pro-oxidant cellular processes. For all three endpoints, all main effects including several interaction terms were retained in the more complex AIC selected models. In the simpler BIC models (Tables S6, S10 and S13†) the main effect "exposure concentration" was not retained in the models fitted to the cellular endpoints (see summary of model fitting in Table S16†), which matches the experimental results on particle sedimentation.

For the ROS related endpoints (H_2DCF-DA and CellROX® Green) the AIC models suggest a significant effect of exposure concentration, as well as interaction between exposure concentration and exposure medium. More generalized, this finding implies that pro-oxidant processes of varying nano-TiO_2 concentrations will differ as a function of the ambient medium. On the other hand, the effect of varying nano-TiO_2 concentrations on membrane damage is simply an additive factor, independent of the respective levels of all the other factors while the impact of the medium will be influenced by the exposure time

and UV treatment and *vice versa*. In more general terms, this implies that the medium itself can affect membrane integrity. Furthermore, we can infer from the fitted models that the effect of UV treatment on all endpoints considered will significantly depend on the exposure medium.

Extracellular H_2O_2 and its utility as biomarker of oxidative stress

To explore the utility of extracellular H_2O_2 as a biomarker of oxidative stress, we first measured abiotic (cell-free) ROS and H_2O_2 concentrations ($c_{H_2O_2}$) in the respective exposure settings to establish the background (medium only) and baseline values (nano-TiO_2 only) of our exposure setup, against which the trends of changes in biotic (in the presence of cells) $c_{H_2O_2}$ can be compared in a subsequent step. Since our measure of cellular oxidative stress is a fluorogenic probe sensitive to ROS in general, we must also consider the possibility that extracellular H_2O_2 is not a good measure of intracellular oxidative stress but rather abiotic ROS in general. Therefore, we also included measurements of abiotic ROS (H_2DCF-DA).

Abiotic ROS (H_2DCF-DA). In both media elevated, above control (0 mg L^{-1} nano-TiO_2) median levels of ROS were only observed at 200 mg L^{-1} nano-TiO_2 (Fig. 4A and B). It has been shown that nano-TiO_2 generates low concentrations of ROS in ambient visible light.[55]

UV treatment of nano-TiO_2 suspensions did not significantly affect ROS levels in lake water, but in the MOPS buffer produced higher median levels of abiotic ROS, most pronounced at 100 and 200 mg L^{-1} nano-TiO_2 ($t = 0$ h and $t = 1$ h, Fig. 2B). This is in agreement with previous findings reporting that the generation of hydroxyl radicals and superoxide anions was higher in ultra-pure MilliQ water than in natural river water.[55]

Abiotic ROS and H_2O_2. The two endpoints for abiotic pro-oxidant processes, ROS (H_2DCF-DA) and H_2O_2 (cyt c biosensor) showed two similarities in trends: (i) in lake water, 200 mg L^{-1} nano-TiO_2 suspensions produced highest levels of H_2O_2 at $t = 1$ h (but, unlike total ROS, it was highest for the entire exposure duration), (ii) in MOPS, 200 mg L^{-1} UV-treated nano-TiO_2 suspensions produced highest levels of H_2O_2 at $t = 0$ h (but decreased to <LOD after 1 h). While UV pre-treatment did not seem to affect ROS in lake water, it greatly increased $c_{H_2O_2}$, especially in the first 10 min. Therefore, abiotic $c_{H_2O_2}$ is a poor measure of abiotic ROS in our setup. Indeed, ROS is a collective term for chemically reactive molecules and when generated by nano-TiO_2 principally includes hydroxyl radicals and superoxide anions, but also comprises H_2O_2 and singlet oxygen.[56,57] However, the DCF method is possibly less sensitive than the cyt c biosensor to measure minute changes in ROS levels due to cells. Nevertheless, this question would merit further, in-depth investigation but is beyond the scope of this article.

The role of particle size on ROS and H_2O_2 generation is another important factor for the understanding of nano-toxicity.[56] However, since nano-TiO_2 immediately formed large agglomerates close to the extreme upper limit of the DLS method in all exposure conditions it seems futile to discuss differences in particle size in relation to pro-oxidant processes observed here. Indeed, this question is worth investigating more comprehensively, but it too goes beyond the scope of this article.

Biotic and abiotic H_2O_2 in lake water and MOPS. The exposure of algae to nano-TiO_2 in lake water did not produce $c_{H_2O_2}$ above the level of unexposed controls (Fig. 5). Nonetheless, the presence of cells reduced $c_{H_2O_2}$ levels obtained for 100 and 200 mg L^{-1} exposures but increased those of 10 and 50 mg L^{-1} exposures with respect to the corresponding abiotic values.

On the other hand, exposure of algae to 50, 100 and 200 mg L^{-1} nano-TiO_2 in MOPS produced higher $c_{H_2O_2}$ levels than in the respective controls. After $t = 1$ h the 10 mg L^{-1} exposure also surpassed the negative control. Similarly, exposure to UV treated nano-TiO_2 surpassed the baseline $c_{H_2O_2}$ levels of controls in the initial 10–20 min of exposure with the 10 mg L^{-1} exposure remaining high until the end of exposure at $t = 1$ h (Fig. 6).

Linking extracellular processes to cellular pro-oxidant processes

Our initial hypothesis stated that peroxide, as a relatively stable subclass of ROS, could serve as a marker for oxidative stress in cells. Based on this premise and on the obtained, continuous measurements of abiotic and biotic (extracellular) $c_{H_2O_2}$ we would thus expect (i) no intracellular oxidative stress and damage in lake water treatments (Fig. 2) and (ii) elevated intracellular ROS levels and membrane damage in cells exposed in MOPS (Fig. 3). In fact, the opposite was observed. Oxidative stress (albeit low values) and membrane damage (up to 15% cells affected) were primarily observed in lake water exposures while there was no evidence of elevated cellular pro-oxidant stress in either controls or treatments conducted in MOPS. Below, we discuss possible explanations for this unexpected finding.

Lake water. In the complex exposure medium such as lake water, the likely presence of trace amounts of metals in lake water samples in combination with DOM/nano-TiO_2-generated H_2O_2 may have facilitated the generation of the more reactive $OH^{\bullet}$ that more rapidly and readily oxidizes biomolecules such as lipids and thereby escaped detection by cyt c, leading to relatively low measured $c_{H_2O_2}$ and higher levels of oxidative stress and membrane damage in exposed cells. In extension, UV treatment induced slightly elevated oxidative stress levels (except at 200 mg L^{-1}) as a consequence of extra $OH^{\bullet}$ emerging from UV generated $c_{H_2O_2}$. The ecotoxicological importance of Haber–Weiss reactions has previously been shown[58] and it has been demonstrated that environmentally relevant concentrations of redox and nonredox active metals enhance intracellular ROS in *C. reinhardtii*, without affecting algal photosynthesis. Alternatively, since DOM is a known ROS scavenger, it is also feasible that DOM competed with the cyt c for H_2O_2 possibly emanating from stressed cells and thereby buffered extracellular $c_{H_2O_2}$. Finally, the observed responses may also be explained by direct physical interactions between nano-TiO_2 and cells. It is well-known that increased ROS and oxidative damage may not only result from a contaminant's direct pro-

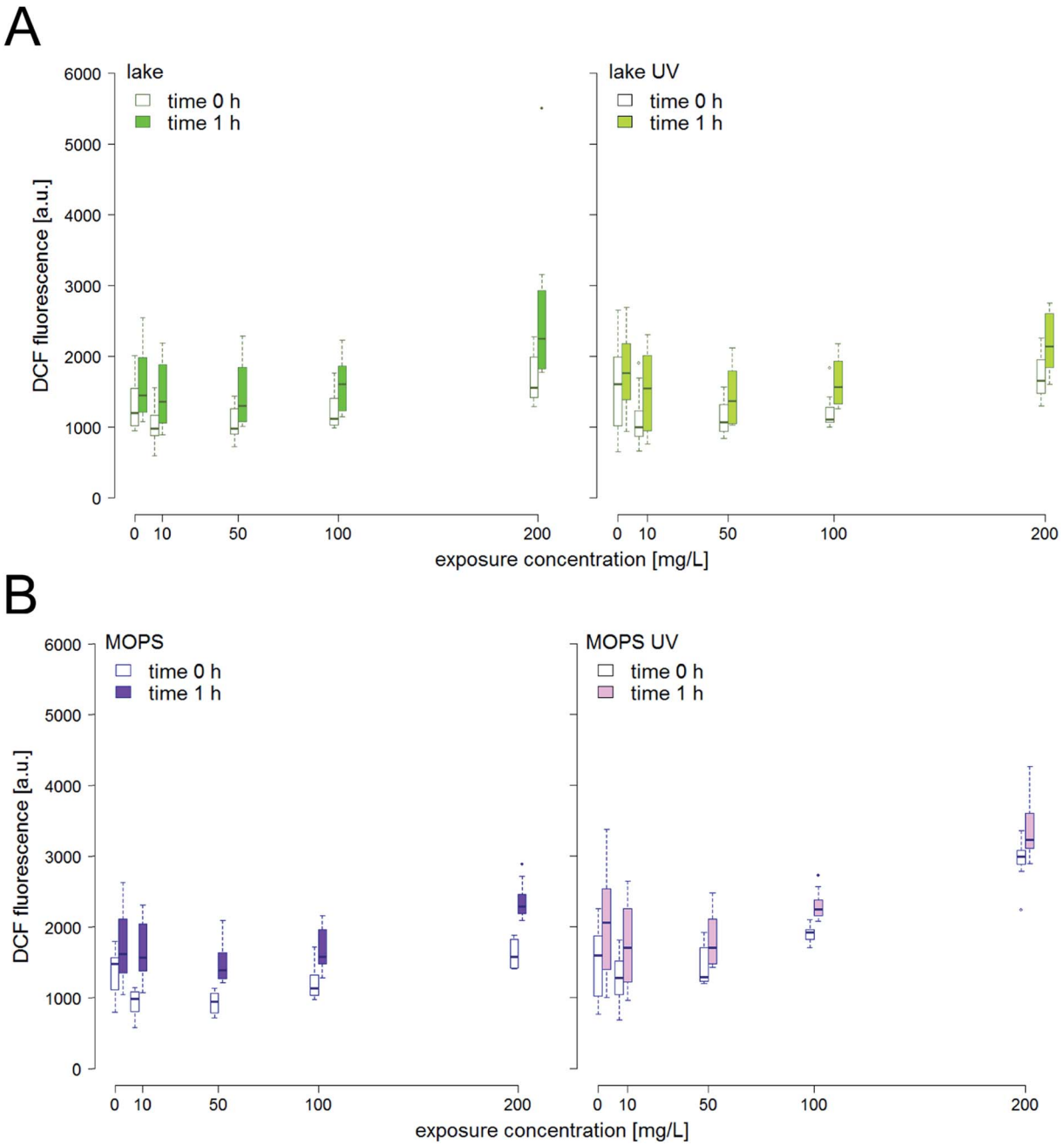

Fig. 4 Tukey box plot of at least triplicates showing abiotic ROS measured as DCF fluorescence at the beginning ($t = 0$ h) and end ($t = 1$ h) of the exposure duration in lake (A) and MOPS (B) at 0 (negative control), 10, 50, 100 and 200 mg L^{-1} nano-TiO_2 without (left plots) and with (right plots) 20 min UVA pre-illumination of suspensions.

oxidant effects. Rather, interactions with a contaminant can lead to some physical injury, which in turn can lead to excess ROS or ROS-generating species.[18] Furthermore, the elevated $c_{H_2O_2}$ measured in cell-free UV pre-treated nano-TiO_2 suspensions in lake water disappeared in the presence of cells, which supports the hypothesis by which free extracellular H_2O_2 react with exposed algae. Plant cells are actually known to consume extracellular H_2O_2 concentrations as high as 10 mM in less than 10 min, as demonstrated by its rapid depletion by *Arabidopsis thaliana* within 8–10 min.[59,60] The proportion of cells with oxidative stress was higher than in non-UV treatments and increased in a concentration dependent manner, except in the [200 mg L^{-1}] UV exposure. Bearing the biotic, non-UV responses in mind, this suggests an additive pro-oxidant effect of H_2O_2 and thus supports the hypothesis of extracellular H_2O_2 reacting with cells in lake water as primary cause over direct cell–particle interactions.

MOPS buffer. In the simple exposure medium MOPS, the results suggest that neither direct particle–cell interactions nor freely diffusing extracellular H_2O_2/ROS present in the medium

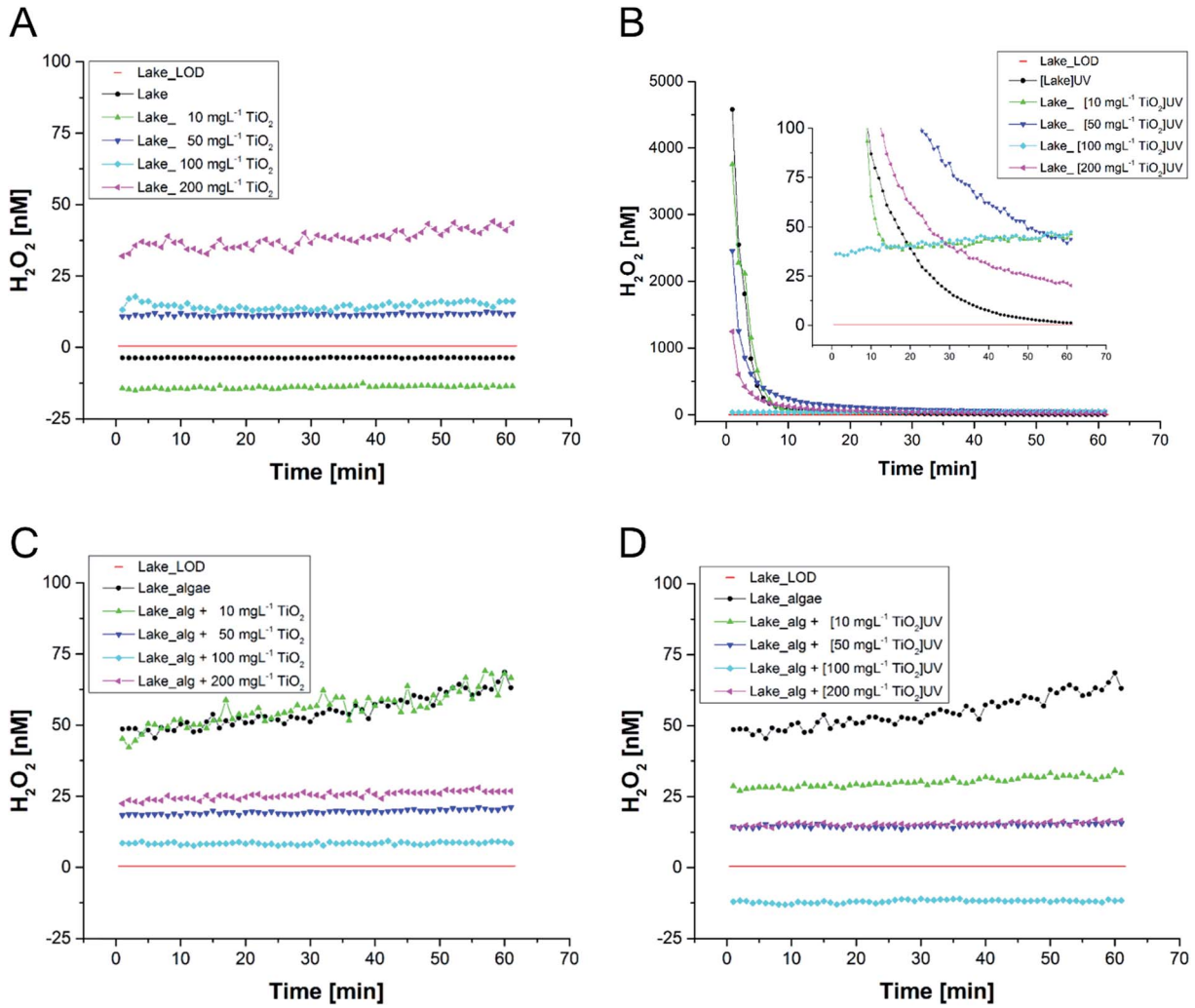

Fig. 5 Average extracellular H_2O_2 ($c_{H_2O_2}$) of at least triplicate measurements produced during 60 min by four nano-TiO_2 concentrations with (B, D) and without UV pretreatment (A, C) in abiotic (A, B) and biotic (C, D) conditions in lake water: nano-TiO_2 only (A), nano-TiO_2 after 20 min UV pre-treatment (B), algae exposed to nano-TiO_2 (C) and algae exposed to UV pre-treated nano-TiO_2 (D). The horizontal red line represents the LOD (239 pM) and the inset in (B) shows a close-up of the 0–100 nM concentration range. Below LOD values are not attributed any meaning and are only included for the sake of completeness.

adversely affected *C. reinhardtii*. In the biotic setting, initial and final $c_{H_2O_2}$ were higher compared to equivalent abiotic conditions for all concentrations but the 10 mg L^{-1} nano-TiO_2 treatment. This implies that algae contributed to the net measured $c_{H_2O_2}$, either through the leaching of intracellular ROS or through reactions of H_2O_2 with the cell surface. On the one hand, if we consider that H_2O_2 is a relatively weak oxidizer[25,61] (particularly in absence of transition metal ions that would enable the formation of the more reactive hydroxyl radical) and both intracellular ROS and membrane integrity were not significantly elevated in exposed cells at the beginning of exposure, the excretion of H_2O_2 by cells is a plausible explanation for the net increase in $c_{H_2O_2}$ at the beginning of exposure. It is known from plants for example that extracellular H_2O_2 concentrations can increase in response to abiotic stressors and environmental pollutants such as metals, pesticides and salt during what is known as the oxidative burst.[62] On the other hand, previous findings showed an accumulation of nano-TiO_2 on the cell surface of microalgae exposed to similar nano-TiO_2 concentrations[43,63–65] and postulated that oxidation occurred through surface-bound ROS which are not free to diffuse into the cell.[66] It is widely acknowledged that proximity or direct contact is a prerequisite for ENP toxicity, without which direct oxidation of cellular components or physical disruption of cell walls and membranes would not occur.[36,66,67] However, assuming this scenario, one would expect oxidative stress or oxidative damage in exposed cells, which was not the case. Abiotic $c_{H_2O_2}$ were higher in UV treatments but all other trends by and large remained the same as in the non-UV treatment. The absence of transition metals in the MOPS buffer may explain why membrane integrity did not degenerate as fast, despite the elevated levels of $c_{H_2O_2}$ both in UV pre-treated and untreated nano-TiO_2 suspensions. Therefore, $c_{H_2O_2}$ excretion by cells seems more plausible.

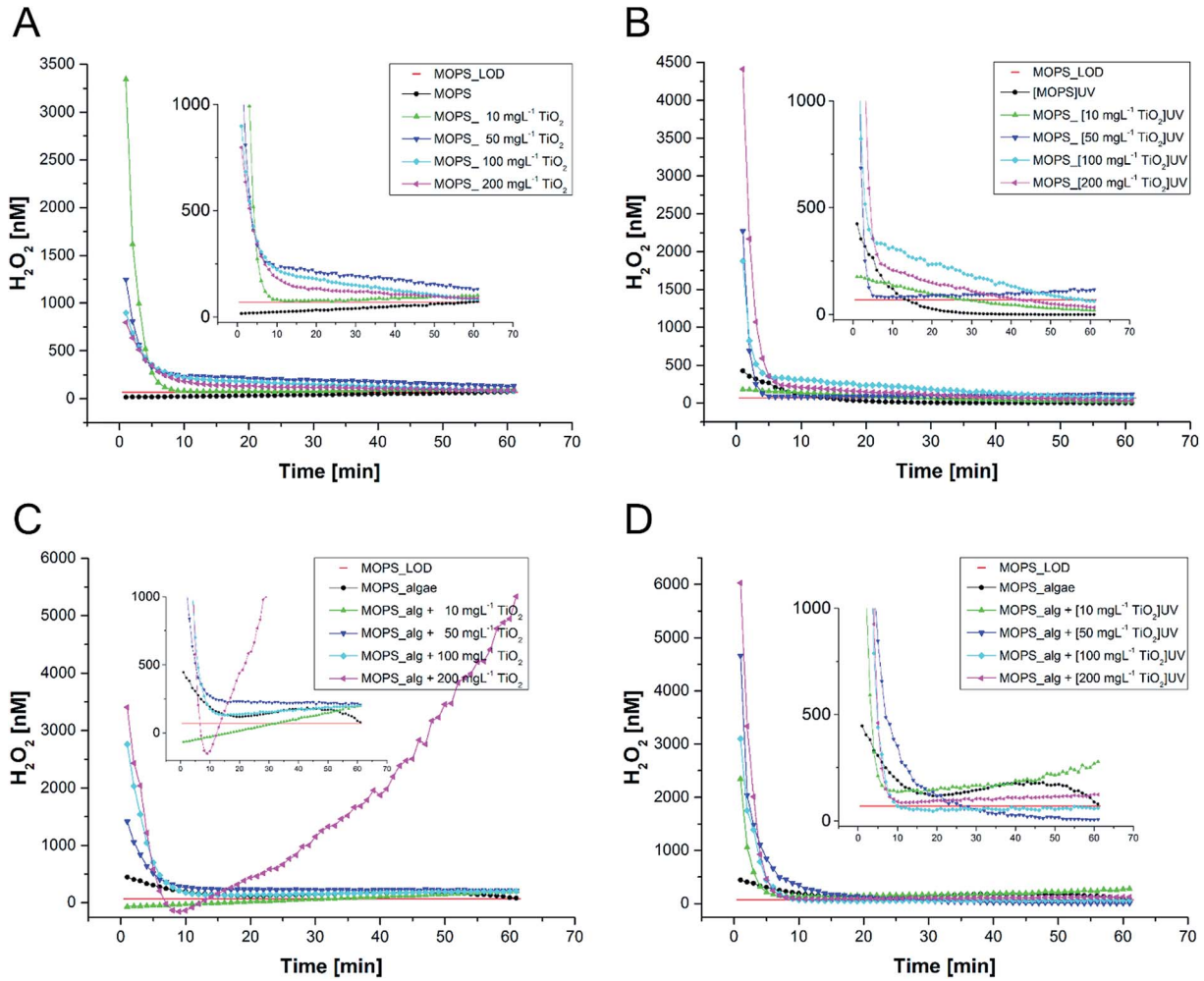

Fig. 6 Average extracellular H_2O_2 ($c_{H_2O_2}$) of at least triplicate measurements produced during 60 min by four nano-TiO_2 concentrations with (B, D) and without UV pre-treatment (A, C) in abiotic (A, B) and biotic (C, D) conditions in the MOPS buffer: nano-TiO_2 only (A), nano-TiO_2 after 20 min UV pre-treatment (B), algae exposed to nano-TiO_2 (C) and algae exposed to UV pre-treated nano-TiO_2 (D). The horizontal red line represents the LOD (37.73 nM) and insets depict enlargements of the respective 0–1000 nM concentration range. Below LOD values are not attributed any meaning and are only included for the sake of completeness.

Conclusion

This is the first in-depth nano-ecotoxicological study to continuously quantify abiotic and biotic nano-TiO_2 – stimulated extracellular H_2O_2 during 1 h exposure of *C. reinhardtii*. It is also the first attempt to link extracellular H_2O_2 to standard nano-ecotoxicological endpoints of cellular pro-oxidant processes. It was found that agglomerated nano-TiO_2 generated cellular pro-oxidant responses, which are significantly modified by the parameters "exposure medium", "exposure time", "UV pre-illumination" as well as "exposure concentrations". Furthermore, extra- and intracellular pro-oxidant processes differed significantly: intracellular oxidative stress increased in conditions where no significant increase in extracellular biotic H_2O_2 was measured and elevated extracellular levels of abiotic H_2O_2 did not point to intracellular oxidative stress. These results suggest that nano-TiO_2 toxicity is not mediated by pro-oxidant processes alone and that extracellular H_2O_2 cannot serve as a marker of cellular oxidative stress and damage in our system. Hence, while measurements of extracellular H_2O_2 provide important additional information on the system under study, the dynamics of H_2O_2 cannot directly serve as a predictor of cellular pro-oxidant processes. These findings are important for ENM hazard assessment and prediction.

Conflict of interest

All authors declare that there are no conflicts of interest.

Acknowledgements

This work was part of the National Research Program 64 on the Opportunities and Risk of Nanomaterials with the project number 406440-131280, funded by the Swiss National Science Foundation. Many thanks are extended to Maurus Thurneysen for support in statistical analyses with *R*.

References

1 T. M. Scown, R. van Aerle and C. R. Tyler, *Crit. Rev. Toxicol.*, 2010, **40**, 653–670.
2 M. N. Moore, *Environ. Int.*, 2006, **32**, 967–976.
3 S. J. Klaine, A. A. Koelmans, N. Horne, S. Carley, R. D. Handy, L. Kapustka, B. Nowack and F. v. d. Kammer, *Environ. Toxicol. Chem.*, 2012, **31**, 3–14.
4 A. Bour, F. Mouchet, J. Silvestre, L. Gauthier and E. Pinelli, *J. Hazard. Mater.*, 2015, **283**, 764–777.
5 A. B. Djurisic, Y. H. Leung, A. M. C. Ng, X. Y. Xu, P. K. H. Lee, N. Degger and R. S. S. Wu, *Small*, 2015, **11**(1), 26–44.
6 N. von Moos, P. Bowen and V. I. Slaveykova, *Environ. Sci.: Nano*, 2014, **1**, 214–232.
7 E. Burello and A. P. Worth, *Nanotoxicology*, 2011, **5**, 228–235.
8 H. Zhang, Z. Ji, T. Xia, H. Meng, C. Low-Kam, R. Liu, S. Pokhrel, S. Lin, X. Wang, Y.-P. Liao, M. Wang, L. Li, R. Rallo, R. Damoiseaux, D. Telesca, L. Mädler, Y. Cohen, J. I. Zink and A. E. Nel, *ACS Nano*, 2012, **6**, 4349–4368.
9 A. Nel, T. Xia, L. Madler and N. Li, *Science*, 2006, **311**, 622–627.
10 A. E. Nel, L. Mädler, D. Velegol, T. Xia, E. M. V. Hoek, P. Somasundaran, F. Klaessig, V. Castranova and M. Thompson, *Nat. Mater.*, 2009, **8**, 543–557.
11 A. L. Neal, *Ecotoxicology*, 2008, **17**, 362–371.
12 T. Xia, M. Kovochich, J. Brant, M. Hotze, J. Sempf, T. Oberley, C. Sioutas, J. I. Yeh, M. R. Wiesner and A. E. Nel, *Nano Lett.*, 2006, **6**, 1794–1807.
13 K. Donaldson, P. H. Beswick and P. S. Gilmour, *Toxicol. Lett.*, 1996, **88**, 293–298.
14 S. J. Soenen, P. Rivera-Gil, J.-M. Montenegro, W. J. Parak, S. C. De Smedt and K. Braeckmans, *Nano Today*, 2011, **6**, 446–465.
15 N. von Moos and V. Slaveykova, *Nanotoxicology*, 2014, **8**, 605–630.
16 D. A. Notter, D. M. Mitrano and B. Nowack, *Environ. Toxicol. Chem.*, 2014, **33**, 2733–2739.
17 N. von Moos, L. Maillard and V. I. Slaveykova, *Aquat. Toxicol.*, 2015, **161**, 267–275.
18 D. R. Livingstone, *Mar. Pollut. Bull.*, 2001, **42**, 656–666.
19 G. Suárez, C. Santschi, O. J. F. Martin and V. I. Slaveykova, *Biosens. Bioelectron.*, 2013, **42**, 385–390.
20 G. Suárez, C. Santschi, V. I. Slaveykova and O. J. F. Martin, *Sci. Rep.*, 2013, **3**, 03447.
21 V. B. Koman, C. Santschi, N. R. von Moos, V. I. Slaveykova and O. J. F. Martin, *Biosens. Bioelectron.*, 2015, **68**, 245–252.
22 V. B. Koman, N. R. von Moos, C. Santschi, V. I. Slaveykova and O. J. F. Martin, *Nanotoxicology*, 2016, 1–29, DOI: 10.3109/17435390.2016.1144826.
23 M. Dynowski, G. Schaaf, D. Loque, O. Moran and U. Ludewig, *Biochem. J.*, 2008, **414**, 53–61.
24 G. P. Bienert, A. L. B. Moller, K. A. Kristiansen, A. Schulz, I. M. Moller, J. K. Schjoerring and T. P. Jahn, *J. Biol. Chem.*, 2007, **282**, 1183–1192.
25 V. Demidchik, *Environ. Exp. Bot.*, 2015, **109**, 212–228.
26 *Free radicals in biology and medicine*, ed. B. Halliwell and J. M. C. Gutteridge, Oxford University Press Inc, 2007.
27 K. Aschberger, C. Micheletti, B. Sokull-Kluttgen and F. M. Christensen, *Environ. Int.*, 2011, **37**, 1143–1156.
28 M. A. Torres, M. P. Barros, S. C. G. Campos, E. Pinto, S. Rajamani, R. T. Sayre and P. Colepicolo, *Ecotoxicol. Environ. Saf.*, 2008, **71**, 1–15.
29 B. Fadeel and A. E. Garcia-Bennett, *Adv. Drug Delivery Rev.*, 2010, **62**, 362–374.
30 A. Weir, P. Westerhoff, L. Fabricius, K. Hristovski and N. von Goetz, *Environ. Sci. Technol.*, 2012, **46**, 2242–2250.
31 Y. Yang, K. Doudrick, X. Y. Bi, K. Hristovski, P. Herckes, P. Westerhoff and R. Kaegi, *Environ. Sci. Technol.*, 2014, **48**, 6391–6400.
32 X. Chen and S. S. Mao, *Chem. Rev.*, 2007, **107**, 2891–2959.
33 O. Carp, C. L. Huisman and A. Reller, *Prog. Solid State Chem.*, 2004, **32**, 33–177.
34 R. X. Cai, Y. Kubota, T. Shuin, H. Sakai, K. Hashimoto and A. Fujishima, *Cancer Res.*, 1992, **52**, 2346–2348.
35 R. Cai, K. Hashimoto, Y. Kubota and A. Fujishima, *Chem. Lett.*, 1992, **21**, 427–430.
36 H. A. Foster, I. B. Ditta, S. Varghese and A. Steele, *Appl. Microbiol. Biotechnol.*, 2011, **90**, 1847–1868.
37 F. Hossain, O. J. Perales-Perez, S. Hwang and F. Román, *Sci. Total Environ.*, 2014, **466–467**, 1047–1059.
38 B. Salieri, S. Righi, A. Pasteris and S. I. Olsen, *Sci. Total Environ.*, 2015, **505**, 494–502.
39 C. A. Linkous, G. J. Carter, D. B. Locuson, A. J. Ouellette, D. K. Slattery and L. A. Smitha, *Environ. Sci. Technol.*, 2000, **34**, 4754–4758.
40 W.-M. Lee and Y.-J. An, *Chemosphere*, 2013, **91**, 536–544.
41 K. Hund-Rinke and M. Simon, *Environ. Sci. Pollut. Res.*, 2006, **13**, 225–232.
42 J. X. Wang, X. Z. Zhang, Y. S. Chen, M. Sommerfeld and Q. Hu, *Chemosphere*, 2008, **73**, 1121–1128.
43 F. M. Li, Z. Liang, X. Zheng, W. Zhao, M. Wu and Z. Y. Wang, *Aquat. Toxicol.*, 2015, **158**, 1–13.
44 E. H. Harris, *The Chlamydomonas Sourcebook - a Comprehensive Guide to Biology and Laboratory Use*, Academic Press, San Diego CA, 2nd edn, 2009.
45 M. Senna, N. Myers, A. Aimable, V. Laporte, C. Pulgarin, O. Baghriche and P. Bowen, *J. Mater. Res.*, 2013, **28**, 354–361.
46 P. J. Neale, P. Bossard and Y. Huot, *Aquat. Sci.*, 2001, **63**, 250–264.
47 P. Hinderliter, K. Minard, G. Orr, W. Chrisler, B. Thrall, J. Pounds and J. Teeguarden, *Part. Fibre Toxicol.*, 2010, **7**, 36.
48 A. Ivask, T. Titma, M. Visnapuu, H. Vija, A. Kakinen, M. Sihtmae, S. Pokhrel, L. Madler, M. Heinlaan, V. Kisand, R. Shimmo and A. Kahru, *Curr. Top. Med. Chem.*, 2015, **15**, 1914–1929.
49 J. H. Priester, P. K. Stoimenov, R. E. Mielke, S. M. Webb, C. Ehrhardt, J. P. Zhang, G. D. Stucky and P. A. Holden, *Environ. Sci. Technol.*, 2009, **43**, 2589–2594.
50 P. Baveye and M. Laba, *Environ. Health Perspect.*, 2008, **116**, A152.
51 C. Perstrimaux, S. Le Faucheur, M. Mortimer, S. Stoll, F. B. Aubry, M. Botter, R. Zonta and V. I. Slaveykova, *Aquat. Geochem.*, 2014, 1–20.

52 A. A. Keller, H. T. Wang, D. X. Zhou, H. S. Lenihan, G. Cherr, B. J. Cardinale, R. Miller and Z. X. Ji, *Environ. Sci. Technol.*, 2010, **44**, 1962–1967.
53 S. P. Yang, O. Bar-Ilan, R. E. Peterson, W. Heideman, R. J. Hamers and J. A. Pedersen, *Environ. Sci. Technol.*, 2013, **47**, 4718–4725.
54 D. Lin, J. Ji, Z. Long, K. Yang and F. Wu, *Water Res.*, 2012, **46**, 4477–4487.
55 M. Planchon, T. Jittawuttipoka, C. Cassier-Chauvat, F. Guyot, A. Gelabert, M. F. Benedetti, F. Chauvat and O. Spalla, *J. Colloid Interface Sci.*, 2013, **405**, 35–43.
56 J. Jiang, G. Oberdörster, A. Elder, R. Gelein, P. Mercer and P. Biswas, *Nanotoxicology*, 2008, **2**, 33–42.
57 M. Cho, H. Chung, W. Choi and J. Yoon, *Water Res.*, 2004, **38**, 1069–1077.
58 I. Szivak, R. Behra and L. Sigg, *J. Phycol.*, 2009, **45**, 427–435.
59 M. I. Gonzalez-Sanchez, L. Gonzalez-Macia, M. T. Perez-Prior, E. Valero, J. Hancock and A. J. Killard, *Plant, Cell Environ.*, 2013, **36**, 869–878.
60 A. Levine, R. Tenhaken, R. Dixon and C. Lamb, *Cell*, 1994, **79**, 583–593.
61 J. M. Burns, W. J. Cooper, J. L. Ferry, D. W. King, B. P. DiMento, K. McNeill, C. J. Miller, W. L. Miller, B. M. Peake, S. A. Rusak, A. L. Rose and T. D. Waite, *Aquat. Sci.*, 2012, **74**, 683–734.
62 S. Bhattacharjee, *Curr. Sci.*, 2005, **89**, 1113–1121.
63 D. M. Metzler, M. Li, A. Erdem and C. P. Huang, *Chem. Eng. J.*, 2011, **170**, 538–546.
64 I. M. Sadiq, S. Dalai, N. Chandrasekaran and A. Mukherjee, *Ecotoxicol. Environ. Saf.*, 2011, **74**, 1180–1187.
65 J. Ji, Z. Long and D. Lin, *Chem. Eng. J.*, 2011, **170**, 525–530.
66 O. K. Dalrymple, E. Stefanakos, M. A. Trotz and D. Y. Goswami, *Appl. Catal., B*, 2010, **98**, 27–38.
67 P. C. Maness, S. Smolinski, D. M. Blake, Z. Huang, E. J. Wolfrum and W. A. Jacoby, *Appl. Environ. Microbiol.*, 1999, **65**, 4094–4098.